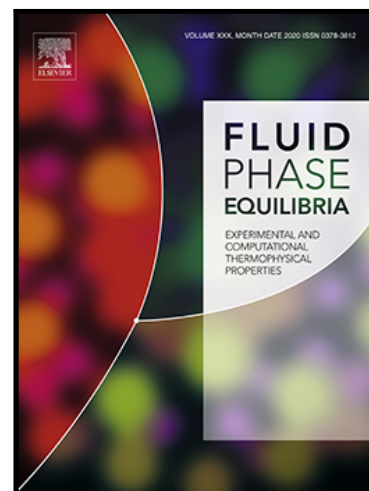


A THEORETICAL STUDY ON THE SIMULTANEOUS
VAPOR-LIQUID AND CHEMICAL EQUILIBRIA IN A HIGHLY
RESTRICTED SYSTEM

Matías J. Molina , S. Belén Rodríguez-Reartes ,
Marcelo S. Zabaloy

PII: S0378-3812(22)00064-4
DOI: <https://doi.org/10.1016/j.fluid.2022.113439>
Reference: FLUID 113439



To appear in: *Fluid Phase Equilibria*

Received date: 23 January 2022
Revised date: 24 February 2022
Accepted date: 2 March 2022

Please cite this article as: Matías J. Molina , S. Belén Rodríguez-Reartes , Marcelo S. Zabaloy , A THEORETICAL STUDY ON THE SIMULTANEOUS VAPOR-LIQUID AND CHEMICAL EQUILIBRIA IN A HIGHLY RESTRICTED SYSTEM, *Fluid Phase Equilibria* (2022), doi: <https://doi.org/10.1016/j.fluid.2022.113439>

This is a PDF file of an article that has undergone enhancements after acceptance, such as the addition of a cover page and metadata, and formatting for readability, but it is not yet the definitive version of record. This version will undergo additional copyediting, typesetting and review before it is published in its final form, but we are providing this version to give early visibility of the article. Please note that, during the production process, errors may be discovered which could affect the content, and all legal disclaimers that apply to the journal pertain.

A THEORETICAL STUDY ON THE SIMULTANEOUS VAPOR-LIQUID AND CHEMICAL EQUILIBRIA IN A HIGHLY RESTRICTED SYSTEM

Matías J. Molina^{1,2} Conceptualization, Methodology, Software, Writing - original draft, Writing - review & editing, S. Belén Rodríguez-Reartes^{1,2} Conceptualization, Methodology, Software, Writing - original draft, Writing - review & editing, Supervision, Funding acquisition, Marcelo S. Zabaloy^{1,2,*} mzabaloy@plapiqui.edu.ar, marcelo.zabaloy@yahoo.com.ar Conceptualization, Methodology, Writing - original draft, Writing - review & editing, Supervision, Funding acquisition

¹Departamento de Ingeniería Química, Universidad Nacional del Sur (UNS), Bahía Blanca, Argentina

²Planta Piloto de Ingeniería Química-PLAPIQUI (UNS-CONICET), Bahía Blanca, Argentina

*Correspondence author

ABSTRACT

In this work, the isomerization reaction of n-butane (C4(2)) to isobutane (iC4(1)) in the absence of other components is studied with the help of a model, in a relatively wide pressure range, both, under single fluid phase conditions and under vapor-liquid equilibrium conditions. In this last case the phase and chemical equilibrium are solved simultaneously. This binary system was chosen, among other considerations, because of the low number of degrees of freedom that it has, according to the phase rule for reactive systems. Such high level of restriction leads to a peculiar behavior that provides interesting insights, in particular on the simultaneous chemical and phase equilibrium. The C4(2) + iC4(1) system is represented in this work by the Soave-Redlich-Kwong equation of state coupled to quadratic mixing rules with binary interaction parameters set to zero. The required computation algorithms were developed in this work. The computed fluid phase equilibrium of this reactive system is a single univariant vapor-liquid equilibrium line. Such line ends at the only reactive vapor-liquid critical point that the system has. Some reactive isochores (or isotherms) were also computed. The obtained computation results show that for this system the conversion can be changed, under certain conditions, just by modifying the overall density, while keeping the temperature and the pressure at constant values.

Keywords: binary mixtures, equation of state, chemical equilibrium, vapor-liquid equilibrium.

1. INTRODUCTION

Isomerization is a chemical reaction in which a molecule becomes another one having the same atoms but arranged in a different way, i.e., the empirical formula is the same for reactant and product. In particular, the n-butane (C4(2)) to isobutane (iC4(1)) isomerization reaction has been used for, e.g., producing iso-butene for synthesizing methyl tertiary butyl ether (MTBE), tertiary butyl alcohol (TBA), isoprene, polyisobutene (PIB) and polyisobutene rubber [1]. Besides, isobutane is used in reactions with C3, C4, and C5 olefins to generate motor fuel alkylate [2].

Indeed, for setting the optimal isobutane production and processing conditions, it would be convenient to have the ability of modeling, at quantitative level, the phase and/or chemical equilibrium conditions of the multicomponent system containing C4(2) and iC4(1), and of modeling the equilibria of the binary subsystems, in particular of subsystem C4(2) + iC4(1).

But, rather than such practical goal of quantitative accuracy, it is our concern here to scrutinize how this binary C4(2) + iC4(1) reactive system behaves, according to a model expected to provide at least qualitatively correct predictions.

The level of simplicity of this binary reactive system could be considered quite high. This is the reason for having chosen it in this work. First, the C4(2) ↔ iC4(1) isomerization reaction is among the simplest possible reactions, since only one reactant and one product are involved (see Eq. (1)). Indeed, during the reaction course, the total number of moles remains invariant, which also adds to the system simplicity. Besides, as it can be expected for many (but not all) isomerization reactions, reactant and product, i.e., C4(2) and iC4(1), are chemically very similar, which implies that a number of their physical properties have similar values, or have the same order of magnitude, e.g., their solubilities in water are very low (which evidences the non-polar nature of either component). Notice that the only structural isomer of C4(2) is iC4(1).

Hence, by choosing the reactive system C4(2) + iC4(1), a number of factors, that would increase the level of complexity of the chemical and phase behavior, are removed, with the goal of gaining a deeper understanding into the behavior of homogeneous or multiphase reactive systems.

Specifically, in this work we study, among other topics, the simultaneous chemical and fluid phase equilibria of the C4(2) + iC4(1) system, mainly for its theoretical interest.

According to the phase rule for reactive systems, the C4(2) + iC4(1) system has only one degree of freedom under liquid-vapor equilibrium (VLE) conditions, and only two degrees of freedom under single fluid phase conditions. Because (among other reasons) of such low number of degrees of freedom, the C4(2) + iC4(1) system could be at first sight considered of low complexity, which should lead to valuable insights on the behavior of highly restricted reactive systems.

Examples of questions that naturally arise when focusing on this reactive binary system are the following:

- Does the C4(2) + iC4(1) VLE locus look similar to that of a pure component?
 - If so: in which ways?
- Are single-phase segments, of reactive C4(2) + iC4(1) isochores, linear in the PT plane, as generally are those of pure components or of non-reactive multicomponent mixtures?
 - ... or due to the isomerization reaction should the isochores show some curvature?

In this work we provide the corresponding answers, among other conclusions. For that, we compute in this work, in a relatively wide pressure range, the binary vapor-liquid equilibrium (VLE) locus of the reactive mixture, which includes a critical point. A number of monophasic reactive isochores and isotherms are also computed. For the calculations, we consider the conditions of phase and chemical equilibria while using the Soave-Redlich-Kwong [3] equation of state (EoS).

2. METHODOLOGY

The isomerization reaction of n-butane (C4(2)) to isobutane (iC4(1)) in the absence of other components is given by Eq. (1).



iC4(1) is labeled as component 1 because it is the lightest (most volatile) component (see Fig. 1).

2.1. Computation of a reactive binary fluid phase equilibrium characteristic map (R-B-CM)

In general, the fluid phase equilibrium characteristic map (CM) of a non-reactive binary (B) system (B-CM) is made of critical and liquid-liquid-vapor lines, and of pure component liquid-vapor equilibrium lines [4]. A point of any of these lines has a single degree of freedom. Such number of degrees of freedom, i.e., one, is also the condition for any point of a line of a reactive (R) binary fluid phase equilibrium characteristic map (R-B-CM).

The calculation of a binary vapor-liquid equilibrium point in presence of one chemical reaction requires solving the set of equations that arises from imposing: (a) the uniformity of temperature and pressure throughout the heterogeneous system, (b) the isofugacity in both phases for each component, and (c) the chemical equilibrium condition for the only reaction taking place in the system. The resulting set of equations is the following:

$$F_1 = P - h_{PVT}(T, x_1, x_2, \tilde{v}_x) \quad (2.1)$$

$$F_2 = P - h_{PVT}(T, y_1, y_2, \tilde{v}_y) \quad (2.2)$$

$$F_3 = \hat{f}_1(T, y_1, y_2, \tilde{v}_y) - \hat{f}_1(T, x_1, x_2, \tilde{v}_x) \quad (2.3)$$

$$F_4 = \hat{f}_2(T, y_1, y_2, \tilde{v}_y) - \hat{f}_2(T, x_1, x_2, \tilde{v}_x) = 0 \quad (2.4)$$

$$F_5 = x_1 + x_2 - 1 \quad (2.5)$$

$$F_6 = y_1 + y_2 - 1 \quad (2.6)$$

$$F_7 = \mu_1(T, y_1, y_2, \tilde{v}_y) - \mu_2(T, y_1, y_2, \tilde{v}_y) \quad (2.7)$$

where P and T are the absolute pressure and temperature of the system, respectively, x_1 and x_2 are the mole fractions of components 1 and 2, respectively, in the fluid phase “x”. y_1 and y_2 are the mole fractions of components 1 and 2, respectively, in the fluid phase “y”. \tilde{v}_x is the molar volume of phase “x” and \tilde{v}_y is the molar volume of phase “y”. Notice that the initial composition of the binary system does not appear in Eqs. (2.1) to (2.7) and consequently does not influence the solution of the system of equations. The function h_{PVT} , which is given by the adopted EoS, states how the absolute pressure

relates to the absolute temperature, molar volume and composition of a given phase. Through exact thermodynamics, the function h_{PVT} imposes the expressions of the component fugacities (\hat{f}_i , $i=1,2$). $\hat{f}_i(T, x_1, x_2, \tilde{v}_x)$ is the fugacity of the i -th component in the “x” phase ($i=1,2$) and $\hat{f}_i(T, y_1, y_2, \tilde{v}_y)$ is the fugacity of the i -th component in the “y” phase. Equations (2.1) and (2.2) imply that the pressure (or temperature) of phase “x” is the same than the pressure (or temperature) of phase “y”. Eqs. (2.3) and (2.4) are the isofugacity conditions for components 1 and 2, respectively. Eqs. (2.5) and (2.6) establish that the sum of the mole fractions of the components must equal unity in the phases “x” and “y”, respectively. Eq. (2.7) is the chemical equilibrium condition for reaction (1) where $\mu_i(T, y_1, y_2, \tilde{v}_y)$ is the chemical potential of the i -th component in the “y” phase. Equivalently, Eq. (2.7) might have been written in terms of the chemical potentials in the “x” phase. This is because the chemical potential of a given component is the same for either phase under phase equilibrium conditions.

The system of seven equations [Eqs. (2.1) to (2.7)] has 8 variables ($P, T, x_1, x_2, y_1, y_2, \tilde{v}_x$ and \tilde{v}_y). Hence, the number of degrees of freedom (DoFs) is one. Thus, this reactive binary two-phase equilibrium is univariant. Hence, a continuous set of solutions to the system of Eqs. (2.1) to (2.7), computed in a temperature range, must contribute to the R-B-CM. In contrast to the case of the system of Eqs. (2.1) to (2.7), a non-reactive binary two-phase equilibrium has 2 DoFs, i.e., it is divariant.

The chemical potential $\mu_i(T, y_1, y_2, \tilde{v}_y)$ has the following expression:

$$\mu_i(T, y_1, y_2, \tilde{v}_y) = \mu_i^0(T) + R \cdot T \cdot \ln \left[\frac{\hat{f}_i(T, y_1, y_2, \tilde{v}_y)}{f_i^0} \right] \quad (3)$$

where R is the universal gas constant and f_i^0 is the fugacity of the i -th component in its standard state at temperature T . In this work, the adopted standard state is the pure component in ideal gas state at the standard pressure (P^0) of 1 bar. Hence, $f_i^0 = 1 \text{ bar}$, which is actually independent of T . $\mu_i^0(T)$ is the chemical potential of the “ i -th” component in its standard state at temperature T , and it is given by:

$$\mu_i^0(T) = \Delta H_{f,i}^0(T_0) - \frac{T}{T_0} [\Delta H_{f,i}^0(T_0) - \Delta G_{f,i}^0(T_0)] + R \int_{T_0}^T \frac{C_{p,i}}{R} dT - RT \int_{T_0}^T \frac{C_{p,i}}{R} \frac{dT}{T} \quad (4)$$

where T_0 is a reference temperature ($T_0=298$ K), $\Delta H_{f,i}^0(T_0)$ is the standard state heat of formation of the i -th component at T_0 (Table 1) and $\Delta G_{f,i}^0(T_0)$ is the standard state Gibbs free energy of formation of the i -th component at T_0 (Table 1). $C_{p,i}$ is the pure component ideal gas (or standard state) constant-pressure heat capacity of the i -th component and it is given by the following equation:

$$\frac{C_{p,i}}{R} = A_i + B_i \cdot T + C_i \cdot T^2 + D_i \cdot T^{-2} \quad (5)$$

The values for the constants in Eq. (5), for C4(2) and iC4(1), are given in the Table 1, together with the values for $\Delta H_{f,i}^0(T_0)$ and $\Delta G_{f,i}^0(T_0)$. These constants are to be used in Eq. (5) with T in Kelvin, and they imply, either for iC4(1) or for C4(2), an almost linear behavior for $C_{p,i}$ versus T , within the wide temperature range considered in this work. The $C_{p,i}$ values for iC4(1) and C4(2) are very similar in such range, being the maximum difference in the order of 3 %.

Table 1: Values for $\Delta H_{f,i}^0(T_0)$ and $\Delta G_{f,i}^0(T_0)$ and for the constants in Eq. (5) [5].

Compound	T_{\max} (K)	A	10^3 B	10^6 C	10^{-5} D	$\Delta H_{f,i}^0(T_0)$ (J/mol)	$\Delta G_{f,i}^0(T_0)$ (J/mol)
Isobutane (1)	1500	1.677	37.853	-11.945	0	-134990*	-21440*
n-Butane (2)	1500	1.935	36.915	-11.402	0	-125790	-16570

*[6]. $T_0=298$ K

The derivation of Eq. (4) is analogous to that of Eq. (13.18) in ref. [5].

Later in this article we will show computed values for the equilibrium constant K_{eq} , which, for any chemical reaction, is given by [5]:

$$\ln(K_{eq}) = \frac{-\Delta G^0(T)}{R \cdot T} \quad (6)$$

where ΔG^0 is the standard Gibbs-energy change of reaction and it depends only on temperature. For the isomerization reaction (1) of n-butane(2) to isobutane(1), ΔG^0 is given by

$$\Delta G^0 = \mu_1^0(T) - \mu_2^0(T) \quad (7)$$

where $\mu_1^0(T)$ and $\mu_2^0(T)$ are the standard state chemical potentials of isobutane(1) and n-butane(2) at temperature T , respectively, and they are calculated using Eq. (4).

As previously stated, a non-reactive binary (B) fluid phase equilibrium characteristic map (CM) (B-CM) is made of pure component VLE lines, and of critical, azeotropic and liquid-liquid-vapor (LLV) lines.

If the binary nature (number of components=2) is imposed as a restriction for a reactive system, then, only one chemical reaction can take place in the system, which indeed must have the effect of transforming one of the components into the other one. For systems as simple as C4(2)+iC4(1), there is only one type of univariant line in a reactive B-CM (R-B-CM), i.e., the binary (reactive) VLE line (only one chemical reaction takes place). Such VLE line corresponds to the system of Eqs. (2.1) to (2.7). A binary reactive system might eventually present also an univariant liquid-liquid equilibrium line.

For the reactive binary system C4(2) +iC4(1), represented by a specific thermodynamic model of the EoS type, with specified parameters values, the following algorithm was devised and used for the computation of its R-B-CM:

- I. Compute all univariant loci (B-CM) for the non-reactive binary system C4(2) +iC4(1) using the methodology of Cismondi and Michelsen [4]. For the studied system (by using the SRK-EoS [3], with quadratic mixing rules (QMRs), $k_{ij}=0$, $l_{ij}=0$), this diagram contains both pure component VLE lines and a single critical line (type I system, [10], Fig. 1).
- II. Compute the left-hand side of Eq. (2.7), i.e, the residual of Eq. (2.7), which equals F_7 , at the $(T, y_1, y_2, \tilde{v}_y)$ conditions of each point of the critical line calculated in step I. The point where the residual equals zero is the reactive critical point (R-CP) of the binary reactive system.
- III. Compute the (univariant) reactive VLE line (R-VLE line, red line, or locus A hereafter, in Fig. 2) starting off from the R-CP and continuing with the help of a numerical continuation method (NCM) [7], [8], solving the set of Eqs. (2.1) to (2.7) at each specified, e.g., temperature, until the calculation is stopped at a preset low enough temperature or pressure (solid phases are not accounted for in this work). The calculated reactive VLE (R-VLE) locus is the R-B-CM of the system.

Indeed, in step I, Eq. (2.7) is ignored.

We have not observed any problems with the initial guess for the system of non-linear algebraic equations (2.1) to (2.7) thanks to the mentioned NCM, which takes advantage of the so-called sensitivity vector. Such vector is computed from the information contained in the last converged point, and used to obtain, through linear extrapolation, a very good initial guess for the next point (of the reactive binary vapor-liquid equilibrium curve) to be computed.

The univariant nature, of the binary reactive vapor-liquid equilibrium, means that the system of equations (2.1) to (2.7) (7 equations, 8 variables), defines a hyper-line in the space of the 8 variables of such system. Imagine that, e.g., T , is regarded as the independent variable, then, the hyper-line will have eight 2D projections where the abscissa is T (including the trivial T versus T projection), i.e., eight 2D curves. At a given value for T , there will be 8 derivative values, each associated to one of the eight 2D curves. Such values are, in a way, the components of the sensitivity vector, whose element corresponding to T (associated to the mentioned trivial projection) has the trivial value, i.e., unity.

When using a NCM, the main problem is to obtain a first converged point of the hyper-line to be computed. We obtained such point, in part from the information on the previously found binary reactive critical point (whose coordinates are P_c , T_c , $x_{1,c}$, $x_{2,c}$, and \tilde{v}_c), by following the next steps: (I) Specification of a variable: set a small enough (negative) value for a temperature step ΔT . Specify the temperature value of the first (non-critical) reactive binary two-phase point to be computed as $T=T_c + \Delta T$. (II) Initialization of the remaining variables: (II.1) set a small enough (positive) value for Δx . (II.2) Set $x_l = (x_{1,c} - \Delta x)$ and $y_l = (x_{1,c} + \Delta x)$. Notice that $(y_l - x_l)/2 = \Delta x$, i.e., Δx is half the difference in component 1 mole fraction, between the vapor and liquid phases. (II.3) Set $x_2 = 1 - x_l$ and $y_2 = 1 - y_l$. (II.4) Set $P = P_c$. (II.5) Solve Eq. (2.1) for \tilde{v}_x . (II.6) Solve Eq. (2.2) for \tilde{v}_y . The previous temperature specification, together with the described initialization strategy for the rest of the

variables, led, without convergence problems, to the first computed (non-critical) reactive binary vapor-liquid equilibrium point.

Appendix B shows that the choice of the PVT thermodynamic model (SRK-EoS) and of the binary interaction parameter values (set to zero) is reasonable, since it provides at least qualitatively correct predictions of the non-reactive iC4(1)+C4(2) VLE, which is acceptable in view of the theoretical nature of the present work. Appendix B also reports the values for the critical coordinates and acentric factor used in this work within the SRK-EoS [3].

2.2. Computation of a single-phase segment of a reactive binary isochore.

A single-phase point of a reactive binary equilibrium isochore (R-IC) corresponds to the following system of equations:

$$P-h_{PVT}(T, y_1, y_2, \tilde{v}_y) = 0 \quad (8.1)$$

$$y_1 + y_2 - 1 = 0 \quad (8.2)$$

$$\mu_1(T, y_1, y_2, \tilde{v}_y) - \mu_2(T, y_1, y_2, \tilde{v}_y) = 0 \quad (8.3)$$

$$\rho_g \tilde{v}_y - y_1 M_{W,1} - y_2 M_{W,2} = 0 \quad (8.4)$$

where ρ_g is the global mass (not molar) density whose specified value defines the R-IC, and $M_{W,i}$ is molecular weight of component “i”. Actually, since components 1 and 2 are isomers, we have that $M_{W,1} = M_{W,2}$. The system of equations (8.1) to (8.4) has two DoFs one of which is spent by setting the value of ρ_g . The initial global composition of the binary system does not play a role in the case of the set of equations (8.1) to (8.4). For the computation of a single-phase segment of a R-IC for the reactive binary system C4(2) +iC4(1), the following algorithm was devised and used in this work:

- I. Specify ρ_g .
- II. Compute the R-B-CM according to section 2.1.
- III. Find a point of the R-VLE locus having one of its phases with a mass density equal to ρ_g . This is a reactive two-phase key point (R-KP) of the R-IC, which indeed satisfies the system of equations (8.1) to (8.4), for the phase of density equal to ρ_g .

- IV. Compute the monophasic segment of the R-IC starting off at the found R-KP and continue with the help of a NCM, until the calculation is completed when a pre-set maximum temperature or pressure is reached. At each point of a single-phase segment of a R-IC, the system of equations (8.1) to (8.4) must be solved, after making a second specification, e.g., the value of T .

2.3. Computation of a single-phase segment of a reactive binary isotherm

To calculate a point of a single-phase segment of a reactive binary equilibrium isotherm, the equation of state (i.e. the pressure-temperature-molar volume-composition relationship), and the chemical equilibrium condition for the isomerization reaction must be satisfied, at the specified value of T . The set of equations that must be solved is the following:

$$P-h_{PVT}(T, y_1, y_2, \tilde{v}_y) = 0 \quad (9.1)$$

$$y_1 + y_2 - 1 = 0 \quad (9.2)$$

$$\mu_1(T, y_1, y_2, \tilde{v}_y) - \mu_2(T, y_1, y_2, \tilde{v}_y) = 0 \quad (9.3)$$

The set of equations (9.1) to (9.3) has two DoFs and one of them is spent by specifying the value of T . Again, the initial composition of the binary system does not play a role in the system of equations (9.1) to (9.3). For the computation of a single-phase segment of a reactive isotherm for the binary system C4(2) + iC4(1), the following algorithm is proposed:

- I. Specify T .
- II. Compute the R-B-CM according to section 2.1.
- III. Find a point of the R-VLE locus having a phase of temperature equal to T . This is a R-KP of the reactive isotherm, since it satisfies Eqs. (9.1) to (9.3). Clearly, at a given T , two R-KPs will be found: one corresponding to the saturated vapor phase and the other to the saturated liquid phase. Each of the two R-KPs is the origin of a particular isothermal single-phase equilibrium reactive segment.
- IV. Compute the monophasic segment of the reactive isotherm starting off at the found R-KP and continue with the help of a NCM, until the calculation is completed when a pre-set maximum (or minimum) pressure is reached. At each

point of a single-phase segment of a reactive isotherm, the set of equations (9.1) to (9.3) must be solved, after making a second specification, e.g., the value of P .

3. STANDARD STATES

As previously stated, Eq. (2.7), which is written in terms of the chemical potentials of the components in the “y” phase, could have been replaced by an analogous equation but written in terms of the chemical potentials of the components in the “x” phase. This naturally brings up the question of whether the choice of the standard states of the system components should be different for phases “y” and “x”. On one hand, the answer is that such standard states can indeed be different, but, in such a case, the values of the two standard chemical potentials, together with the values of the two standard fugacities, for the component under consideration, must comply with certain restriction (Eq. (10)). On the other hand, the answer is completed by stating that it is unnecessary, and hence impractical, to choose different component standard states for phases “y” and “x”.

The chemical potential of a given component should be calculated, for simplicity, using a unique standard state in Eq. (3), regardless the nature of the phase under consideration. Thus, if, e.g., the chosen standard state is, for a given component, the pure component in ideal gas state at the standard pressure, then, such standard state would be used both, for a vapor phase and for a liquid phase.

If it were anyway decided to use more than one standard state for a given component, say, standard states A and B, then, they would be connected, at given temperature, by the following equation,

$$\mu_{i,B}^0 = \mu_{i,A}^0 + R \cdot T \cdot \ln \left[\frac{\hat{f}_{i,B}^0}{\hat{f}_{i,A}^0} \right] \quad (10)$$

where $\mu_{i,A}^0$ and $\mu_{i,B}^0$ are the chemical potentials, and $\hat{f}_{i,A}^0$ and $\hat{f}_{i,B}^0$ the fugacities, of component “i” in standard states A and B, respectively (see, e.g., Eq. 2-46 in reference [9]).

To fix ideas, standard state A could, e.g., be the pure real liquid at standard pressure and at temperature T , while standard state B could, e.g., be the pure real solid also at

standard pressure and at temperature T . Besides, standard states A or B do not necessarily have to correspond to pure components.

Eq. (10) is a relationship between two standard states which comes from exact thermodynamics. It establishes that the thermodynamic properties of two different standard states are interrelated. In this way, for a given component, different standard states are not mutually independent. Notice that restriction (10) is to be met at every temperature.

If we had written Eq. (2.7) in terms of the chemical potentials of the components in the “x” phase, instead of writing it in terms of the chemical potentials of the components in the “y” phase, then, we would have still chosen, in this work, for practical reasons, the pure component in ideal gas state, at standard pressure, as the standard state for either component in the binary system.

4. RESULTS

In this section the calculation results for the vapor-liquid and single-phase equilibria related to the isomerization reaction $C4(2) \leftrightarrow iC4(1)$ in the absence of other components are shown. As previously stated, the volumetric and phase behavior of this system were modeled through the SRK-EoS coupled to quadratic mixing rules (QMRs). The values used for the binary interaction parameters (BIPs) are $k_{ij}=0$ (attractive BIP) and $l_{ij}=0$ (repulsive BIP). See Appendix B for more information. If the isomerization reaction is ignored, a type I phase behavior is obtained through application of the algorithms of ref [4], for the (regarded as non-reactive) $C4(2) + iC4(1)$ system, according to the classification of Scott and Van Konynenburg [10]. Figure 1 shows the pressure – temperature projection of the B-CM of the $C4(2) + iC4(1)$ non-reactive system. Figure 1 just contains one binary vapor-liquid critical curve (solid black curve), which continuously connects the critical points of the two pure components. Figure 1 also shows the VLE curves of the pure components (solid blue and green curves) that start at the critical points of the pure components and extend indefinitely towards low temperatures and pressures.

Figure 2 shows the pressure - temperature projection of the B-R-CM of the $C4(2) + iC4(1)$ reactive system. Figure 2 shows a single univariant VLE line (red line, Fig. 2) that starts at the single reactive critical point of the system and extends indefinitely

towards low temperatures and pressures. This peculiar behavior is due to the unique degree of freedom of the reactive binary VLE (R-B-VLE). The reactive VLE line in Fig. 2 looks as a (non-reactive) pure component VLE line. However, at given T , the vapor phase composition (red curve, Fig. 4) differs from the liquid phase composition (blue curve, Fig. 4). Besides, the composition of a given phase changes when T is changed (Fig. 4). Figure 3 shows the pressure – temperature projection of the B-R-CM along with the B-CM of the $C4(2) + iC4(1)$ system.

In Fig. 2 (and in the red curve of Fig. 3) it is implied that the reactive system has been set fully free to reach equilibrium (absence of kinetic constraints). In such a case, the pure component (non-reactive) VLE curves are metastable (dashed blue and green curves, Fig. 3), as it is the (non-reactive) binary critical line (except for the reactive critical point - black circle - in Figs. 2 and 3, which is stable). The pure component VLE curves metastability implies that the pure component SRK-EoS parameters have been obtained from (regarded as) metastable experimental information (critical (T , P) coordinates and acentric factor, Appendix B).

Figure 4 presents the temperature – composition projection of the B-R-CM of the $C4(2) + iC4(1)$ system. The temperature-composition relationships for the saturated vapor (y_l) and liquid (x_l) of the B-R-CM are shown in red and blue colors in the Fig. 4, respectively. It is observed that the mole fractions y_l and x_l decrease as T increases. The insert in Fig. 4 is a zoom of the critical region, where the curves become flat. Our calculation algorithm is especially robust in the critical region due to the implemented NCM. Since y_l (red line) is always greater than x_l (blue line in Fig. 4), we conclude that in this binary reactive system component 1 ($iC4(1)$) is more volatile than component 2 ($C4(2)$). This is consistent with what could be expected from looking at Fig. 3. The blue curve in Fig. 3 ($iC4(1)$) is above the green curve ($C4(2)$), i.e., $iC4(1)$ would be more volatile than $C4(2)$. This criterion is always applicable under the assumption that the system does not present azeotropes. The validity of such assumption cannot be verified from just looking at the pure component VLE curves.

Figure 5 presents the pressure-composition projection of the computed vapor-liquid equilibrium locus of the reactive system $C4(2) + iC4(1)$. Again, the insert in Fig. 5 facilitates the visualization of the critical region. Notice that Figs. 4 and 5 are different

projections of the same thermodynamic object (which is shown in 3D in Fig. 9a). It is important to emphasize that Fig. 4 is not a constant pressure diagram, and that Fig. 5 is not a constant temperature diagram.

Figure 6 shows the logarithm of the computed equilibrium constant (K_{eq}) of the isomerization reaction of n-butane(2) to isobutane(1) versus the reciprocal of temperature. K_{eq} was calculated at a given temperature from Eq. (6). The relationship between the logarithm of K_{eq} and the reciprocal of temperature is almost linear in Fig. 6. Furthermore, when the temperature increases the equilibrium constant decreases, therefore, this isomerization reaction, Eq. (1), is exothermic under standard conditions [5].

Figure 7 shows the pressure - temperature projection of two single-phase segments of different reactive isochores (R-ICs) for the C4(2) + iC4(1) system. These single-phase segments start at the same point in the PT projection of locus A (point α in Fig. 7) but their global densities are different. The mono-phasic segment of the R-IC of $\rho_g=432.4454$ g/l is of the liquid type, while the one of the R-IC of $\rho_g=30.9525$ g/l is of (homogeneous) vapor type. Furthermore, for the homogeneous segments of the R-ICs, Fig. 7 shows that the pressure is roughly a linear function of temperature, as it generally happens for stable pure components. The (not shown) composition is variable along a single-phase segment of a R-IC. The P vs. T projection of the biphasic segments of the R-ICs fall over locus A, and extend from point α to lower temperatures and pressures. At a given temperature T , less than T_α , the two R-ICs of Fig. 7 differ in vaporized fraction and in equilibrium global composition. At $T < T_\alpha$, the vaporized fraction can be easily computed from the set R-IC global density and the known phase densities at the specified T (Fig. 8, Eq. (13.1)). Once the vaporized fraction is known, the equilibrium global composition can be computed through component mass balances which make use of the phase compositions known at the specified T (Fig. 4, Eq. (13.2)). The corresponding equations are presented later in this article. They are Eqs. (13.1), (13.2) and (13.4).

Figure 8 shows the pressure vs. saturated mass density projection of the computed B-R-CM for the C4(2) + iC4(1) system and it also presents several calculated reactive

isotherms. In Fig. 8, the blue line is a saturated liquid locus and the red line is a saturated vapor locus. In Fig. 8 the subcooled liquid region lies above the blue line, the superheated vapor region above the red line and the vapor-liquid equilibrium region below the blue and red lines. At temperatures below the critical temperature of the reactive mixture ($T_c=413.16$ K), each reactive isotherm has three different segments: a biphasic segment and two monophasic segments. A homogeneous liquid segment begins at a point on the blue line and extends to high pressures, while a given homogeneous vapor segment starts at a point on the red line and extends towards low pressures. A vapor-liquid segment at given T in Fig. 8 extends between the starting points at same T of two single-phase segments and it is a horizontal tie-line in the pressure - density projection of the R-VLE. The isotherm passing through the reactive critical point (R-CP) ($T=413.16$ K) has a unique single-phase segment which extends from low to high pressures, and presents, at the R-CP, an horizontal (not shown) tangent line and an inflection point, as in the case of pure component critical isotherms. The two reactive isotherms at temperatures greater than the reactive critical temperature (i.e., at $T > 413.16$ K) extend from low to high pressures under single-phase conditions, just as pure component isotherms do at reduced temperatures greater than unity. In conclusion, all isotherms shown in Fig. 8 qualitatively behave, in the projection of Fig. 8, as those of a pure component.

In Fig. 9a, the composition – temperature – pressure projection of the B-R-CM for the C4(2) + iC4(1) system is shown. Figure 9a also includes six of the isotherms plotted in Fig. 8. Again, in Fig. 9a, the blue line is the saturated liquid locus and the red line is the saturated vapor locus.

Figure 9b shows the projections of the thermodynamic objects in Fig. 9a onto the pressure-composition plane, with the addition of two isotherms of temperature greater than the reactive critical temperature. Figure 9c is a zoom of Fig. 9b. In Fig. 9b, the composition variation with pressure, at constant temperature, is more noticeable at higher pressures (reactive subcooled liquid or supercritical fluid) than at lower pressures (superheated vapor, or gaseous, reactive fluid). Indeed, the pressure range for the superheated vapor at subcritical temperatures is, in Fig. 9b narrower than the pressure range for the subcooled liquid (also at subcritical temperatures). The horizontal segments in Fig. 9b are the vapor-liquid tie lines.

Consider, e.g., the 350 K reactive isotherm in Fig. 9c. Its high pressure (liquid) branch seems to meet both, the red line and the blue line. Similarly, its low pressure (vapor) branch also seems to meet the red and blue lines. Inspection of Fig. 9a reveals that at 350 K only two out of the four mentioned meeting points are not spurious: the liquid branch only meets the blue line, while the vapor branch only meets the red line (Fig. 9a).

An isotherm such as the 430 K isotherm in Fig. 9c clearly shows that, in general, under homogeneity conditions, the composition and the temperature cannot be kept simultaneously constant while changing the pressure (which is indeed possible in non-reactive homogeneous binary or multicomponent systems).

We see in Figs. 9b and 9c that at set pressure, under homogeneity conditions, as temperature increases the mole fraction of component 1 decreases. This behavior would have been predicted from a preliminary analysis based on Fig. 6, which tells that at higher temperature the lower equilibrium constant for reaction (1) would imply a shift towards the reactant C4(2), i.e., towards lower component 1 concentration.

It can be shown that

$$z_1 = \frac{z_1^0 + \nu_1 \cdot \zeta^*}{1 + (\nu_1 + \nu_2) \cdot \zeta^*} \quad (11.1)$$

and

$$z_2 = \frac{z_2^0 + \nu_2 \cdot \zeta^*}{1 + (\nu_1 + \nu_2) \cdot \zeta^*} \quad (11.2)$$

where z_i is the global mole fraction, and ν_i the stoichiometric coefficient, both for component “i”. Superscript ⁰ on z_i means “initial”. ζ^* is the extent of reaction (ζ) relative to the initial total number of moles (n_0^T) ($\zeta^* = \zeta/n_0^T$). ζ^* is independent of the system size. See the detailed derivation of equations (11.1) and (11.2) in Appendix A. Since $\nu_1 = 1$ and $\nu_2 = -1$ in reaction (1), then, from Eqs. (11.1) and (11.2), we write,

$$z_1 = z_1^0 + \zeta^* \quad (12.1)$$

$$z_2 = z_2^0 + (-1) \zeta^* \quad (12.2)$$

Notice that $z_1 + z_2 = 1$ and $z_1^0 + z_2^0 = 1$.

Figure 10 shows a set of equilibrium isotherms, for the initial global composition $z_{iC4}^0 = z_1^0 = 0.60$, in their ξ^* vs. overall mass density (g/l) projection. For instance, at an overall density of 600 g/l and 390 K, the equilibrium is monophasic (Fig. 8). Such couple of specifications make possible to solve the set of equations (8.1) to (8.4) for the unknown variables, in particular for y_1 , which equals the equilibrium global composition z_1 (since there is only one phase), which makes also possible to obtain ξ^* from Eq. (12.1), at the specified z_1^0 , as shown in Fig. 10. If the global density specification corresponds to a VLE situation, e.g., 200 g/l and 390 K (Fig. 8), it is also possible to compute ξ^* , although in a slightly more complicated way, by solving the next set of equations:

$$\frac{1}{\rho_g} - \Phi_x \cdot \frac{\tilde{v}_x}{M_W} - \Phi_y \cdot \frac{\tilde{v}_y}{M_W} = 0 \quad (13.1)$$

$$z_1 - \Phi_x \cdot x_1 - \Phi_y \cdot y_1 = 0 \quad (13.2)$$

$$z_1 - z_1^0 - \xi^* = 0 \quad (13.3)$$

$$\Phi_x + \Phi_y - 1 = 0 \quad (13.4)$$

where Φ_x and Φ_y are the phase mole fractions of the liquid phase and of the vapor phase, respectively, and M_W is the molecular weight of either phase, since both phases have the same molecular weight. This is because any mixture of C4(2) and iC4(1) has the molecular weight of C4(2), or of iC4(1), since they are isomers. z_1^0 and ρ_g are, as in Fig. 10, considered to be known value parameters of the system of equations (13.1) to (13.4). At set T , also \tilde{v}_x , \tilde{v}_y , x_1 and y_1 are known value parameters obtained from the B-R-CM (system of Eqs. (2.1) to (2.7)); thus, from the set of Eqs. (13.1) to (13.4) the values for Φ_x , Φ_y , z_1 and ξ^* are calculated.

When at given z_l^0 we specify the temperature T , and the overall mass density ρ_g , for our two-phase reactive (closed) system, we are actually applying Duhem's Theorem [5]. It states that, on top of the initial composition, two variables are to be fixed to completely define the equilibrium state of the system. In our case such two variables cannot be both intensive, since our binary two-phase system has just one degree of freedom according to the phase rule for reactive systems. Hence, once the temperature T is set (intensive variable), then, we must specify a global variable, e.g., Φ_x or ζ^* or ρ_g , etc. The value of ρ_g is the global variable specification choice we have made, when solving the system of Eqs. (13.1) to (13.4), to generate Fig. 10.

In Fig. 10, for a set temperature, for example $T=350$ K, starting from the isotherm monophasic liquid region (located to the right of the blue curve, high mass densities), and decreasing the density, then, ζ^* increases until the reactive bubble points curve (blue curve in Fig. 10) is reached. Within the heterogeneous region, ζ^* remains (at $T=350$ K) approximately constant as the global mass density decreases, but increases rapidly when approaching from the right the reactive dew points curve (red curve). If, at 350 K, starting at the red curve, the mass density is reduced further, then, the fluid becomes a homogeneous vapor, and ζ^* increases slightly. This behavior is observed in Fig. 10 for all the isotherms that have a two-phase segment. The critical isotherm ($T_c=413.16$ K) is tangent both, to the red and blue lines, in Fig. 10, at the reactive critical point. For the reactive critical isotherm, ζ^* increases almost linearly with the decrease in the mass density of the mixture. Figure 10 shows that the reactive isotherm of 430 K has no two-phase segment (as already known from, e.g., Fig. 9c). Such isotherm shows an increase in ζ^* as the density decreases (Fig. 10).

It is worth noting that the reactive critical point (point where the red and blue lines meet in Fig. 10) does not correspond to the global minimum of the continuous curve obtained from the union of the blue and red curves in Fig. 10. Otherwise, the R-CP is slightly shifted to the left of the global minimum, as shown Fig. 11 for which the ζ^* and density ranges are narrower than for Fig. 10.

In Fig. 11, the reactive critical isotherm ($T_c=413.16$ K) and the reactive isotherm that goes through the already mentioned global minimum ($T^*=412.31$ K) are shown. In this figure it is clearly observed that the reactive critical point is located to the left of the global minimum. The T^* isotherm has a heterogeneous segment and two homogeneous segments whereas the isotherm at T_c only has a point, i.e., the reactive critical point, in common with the heterogeneous region.

At 350 K, Fig. 10 clearly shows that the saturated liquid and vapor phases differ in their ξ^* values. This is indicative, on one hand, of the difference in composition for the two phases (Eq. (12.1)), and, on the other hand, of the fact that the conversion can be changed by modifying just the total volume of the system, while keeping constant both, the temperature and the pressure (since the saturated liquid and the saturated vapor have not only the same temperature but also the same pressure, due to the single degree of freedom available to the VLE of this binary reactive system).

Figure 12 shows, at saturation, the ξ^* (extent of reaction relative to the initial total number of moles) versus temperature for a set of values of the iC4(1) initial global mole fraction (z_1^0). In Fig. 12, the blue lines are saturated liquid loci and the red lines are saturated vapor loci. For a set temperature, ξ^* (at saturation) increases as the initial mole fraction of iC4(1) decreases. Figure 12 also shows that for certain values of z_1^0 , ξ^* may have negative values, in which case C4(2) is produced from iC4(1) in reaction (1), under saturation conditions.

At, e.g., $z_1^0=0.9$, it is possible to find in Fig. 12 a value for T at which the saturated vapor has $\xi^* > 0$, while the saturated liquid has $\xi^* < 0$. This means that, at constant temperature and pressure, the reaction can be made to fluctuate between C4(2) production and iC4(1) production, just by changing the global molar volume in an oscillatory way, going back and forth from the saturated liquid to the saturated vapor.

All of the saturated liquid loci shown in Fig. 12 present the same shape. The same is observed for all the saturated vapor loci. In other words, the saturated liquid loci (or the saturated vapor loci), for two different values of z_1^0 , are separated one from the other by a constant vertical distance. The reasons for this behavior are explained as follows.

Let $z_{1,A}^0$ and $z_{1,B}^0$ be two different global initial mole fractions of iC4(1) for which we want to compute the saturated vapor ζ^* . At given T , from the Eq. (12.1), we write:

$$z_1 = z_{1,A}^0 + \zeta_A^* \quad (14.1)$$

$$z_1 = z_{1,B}^0 + \zeta_B^* \quad (14.2)$$

In Eqs. (14.1) and (14.2) the value of z_1 is the same since $z_1 = y_1$ for the computation of the saturated vapor ζ^* , where y_1 becomes determined just by the specified temperature (Fig. 4). By subtracting Eq. (14.2) from Eq. (14.1), we obtain:

$$0 = (z_{1,A}^0 - z_{1,B}^0) + (\zeta_A^* - \zeta_B^*) \quad (15)$$

By solving Eq. (15) for ζ_B^* , we obtain,

$$\zeta_B^* = (z_{1,A}^0 - z_{1,B}^0) + \zeta_A^* \quad (16)$$

Eq. (16) indicates that the saturated vapor ζ_B^* differs from the saturated vapor ζ_A^* , at the set T , by the constant $(z_{1,A}^0 - z_{1,B}^0)$ which is independent of T . This implies that the curve for the sat. vap. ζ_B^* is shifted by the constant $(z_{1,A}^0 - z_{1,B}^0)$ from the curve for the sat. vap. ζ_A^* .

The same can be done for the bubble point curve, obtaining the same result. Since in Fig. 12 the difference in the z_1^0 value, between consecutive curves of a given type, e.g., saturated vapor, equals 0.1, a given curve is vertically shifted from a consecutive curve of the same nature (sat. vap. or sat. liq.) by a distance equal to 0.1, in agreement with Eq. (16).

5. REMARKS AND CONCLUSIONS

In this work, the fluid phase equilibria of the binary system n-butane (C4(2)) + isobutane (iC4(1)), subject to the isomerization reaction $C4(2) \leftrightarrow iC4(1)$, was studied on a theoretical level, with the help of the SRK-EoS model coupled to quadratic mixing rules used with binary interaction parameters set to zero.

The computed fluid phase equilibrium characteristic map (CM) of the binary (B) reactive (R) system (R-B-CM) happens to be made of only a single (univariant) reactive

vapor-liquid equilibrium (VLE) line whose Pressure-Temperature (PT) projection (Fig. 2) resembles the one of the vapor-liquid line of a pure component. The pressure-density (P ρ) projection of the reactive binary VLE (Fig. 8) also looks as that of a pure component. The binary VLE is univariant because of the presence of the isomerization reaction, according to the phase rule for reactive systems. A single invariant reactive binary vapor-liquid critical point has also been computed.

Monophasic equilibrium segments, and VLE segments, of reactive isochores and isotherms, for the reactive binary system C4(2) + iC4(1), were also computed. The binary isotherms have the same qualitative behavior than those of a pure component in their P ρ projections (Fig. 8). Due to the highly restricted nature of the reactive C4(2) + iC4(1) system, all equilibrium isotherms of interest can be seen at once in a single pressure-composition diagram (Fig. 9b).

Monophasic segments of computed reactive isochores (Fig. 7) have a linear behavior in the PT plane, as it is generally the case for pure components; while VLE reactive isochore segments are indeed coincident with the proper portion of the reactive VLE curve, also in the PT plane.

All previous conclusions were drawn from computations performed without specifying the system initial composition. Such calculations were performed by applying the computation algorithms proposed in this work.

One of the reactive equilibrium diagrams computed in this work for a specified initial composition (Fig. 10), shows that the reaction extent, and hence the conversion, can be changed under certain conditions just by modifying the overall density, while keeping the temperature and the pressure at constant values. Such conditions are those under which the reactive VLE occurs.

In conclusion, the present theoretical study for the relatively simple case of a binary isomeric reactive system (C4(2) + iC4(1)), carried out for quite wide pressure and temperature ranges, has led us to interesting insights on the behavior of reactive homogeneous or multiphase systems.

List of symbols

$C_{p,i}$ pure component ideal gas (or standard state) constant-pressure heat capacity of the i -th component

\hat{f}_i	fugacity of the i-th component in a given phase
f_i^0	fugacity of the i-th component in its standard state
$\Delta G_{f,i}^0$	standard state Gibbs free energy of formation of the i-th component
$\Delta H_{f,i}^0$	standard state heat of formation of the i-th component
K_{eq}	equilibrium constant
$M_{W,i}$	molecular weight of the i-th component
n_i	number of moles of the i-th component
n_i^0	initial number of moles of the i-th component
n_T^0	initial total number of moles
n_T	total number of moles
P	absolute pressure
P^0	standard absolute pressure
R	universal gas constant
T	absolute temperature
T_0	reference absolute temperature
x_i	mole fraction of component 'i' in the "x" phase
y_i	mole fraction of component 'i' in the "y" phase
z_i^0	initial global mole fraction of the i-th component
z_i	global mole fraction of the i-th component

List of acronyms

B	binary
B-CM	non-reactive binary (B) fluid phase equilibrium characteristic map (CM)
C4(2)	n-butane
DoFs	degrees of freedom
EoS	equation of state
iC4(1)	isobutane
LLV	liquid-liquid-vapor equilibrium
NCM	numerical continuation method
QMRs	quadratic mixing rules
R-B-CM	reactive (R) binary (B) fluid phase equilibrium characteristic map (CM)
R-CP	reactive critical point
R-IC	reactive isochore
R-KP	reactive two-phase key point
R-VLE	reactive vapor-liquid equilibrium
SRK	Soave-Redlich-Kwong (equation of state)
VLE	vapor-liquid equilibrium

Greek symbols

Φ_x	phase mole fraction of phase "x"
Φ_y	phase mole fraction of phase "y"

μ_i	chemical potential of the i-th component
μ_i^0	chemical potential of the “i-th” component in its standard state
ν_i	stoichiometric coefficient of the i-th component
ξ	extent of reaction
ξ^*	extent of reaction relative to the initial total number of moles
ρ_g	global mass density
\tilde{v}_x	molar volume of phase “x”
\tilde{v}_y	molar volume of phase “y”

CREDIT AUTHOR STATEMENT

Matías J. Molina: Conceptualization, Methodology, Software, Writing - Original Draft, Writing - Review & Editing. **S. Belén Rodríguez-Reartes:** Conceptualization, Methodology, Software, Writing - Original Draft, Writing - Review & Editing, Supervision, Funding acquisition. **Marcelo S. Zabaloy:** Conceptualization, Methodology, Writing - Original Draft, Writing - Review & Editing, Supervision, Funding acquisition.

Declaration of interests

The authors declare that they have no known competing financial interests or personal relationships that could have appeared to influence the work reported in this paper.

ACKNOWLEDGEMENTS

We gratefully acknowledge the financial support provided by the Argentinean institutions Consejo Nacional de Investigaciones Científicas y Tecnológicas de la República Argentina (CONICET, Grant # PIP-11220150100918CO), Agencia Nacional de Promoción Científica y Tecnológica (ANPCyT, Grant # PICT-2017-1235) and Universidad Nacional del Sur (UNS, Grant # PGI-24/M169).

APPENDIX A. Relationship between the global mole fractions (z_i) and the extent of reaction relative to the initial total number of moles (ξ^*).

Let ξ be the extent of the isomerization reaction (1), v_1 and v_2 the stoichiometric coefficients of iC4(1) and C4(2) in such reaction, respectively, and n_1^0 and n_2^0 the initial number of moles of iC4(1) and C4(2), respectively. The number of moles of each component as a function of the extent of reaction is given by:

$$n_1 = n_1^0 + v_1 \cdot \xi \quad (\text{A.1})$$

$$n_2 = n_2^0 + v_2 \cdot \xi \quad (\text{A.2})$$

Where n_1 and n_2 are the numbers of moles of iC4(1) and C4(2) corresponding to a given extent of reaction ξ , respectively. By dividing both members of Eqs. (A.1) and (A.2) by the initial total number of moles n_T^0 ($n_T^0 = n_1^0 + n_2^0$), we obtain,

$$\frac{n_1}{n_T^0} = \frac{n_1^0}{n_T^0} + v_1 \cdot \frac{\xi}{n_T^0} \quad (\text{A.3})$$

$$\frac{n_2}{n_T^0} = \frac{n_2^0}{n_T^0} + v_2 \cdot \frac{\xi}{n_T^0} \quad (\text{A.4})$$

By multiplying and dividing the left-hand sides of Eqs. (A.3) and (A.4) by the total number of moles n_T corresponding to ξ ($n_T = n_1 + n_2$), we write:

$$z_1 \cdot r_N = z_1^0 + v_1 \cdot \xi^* \quad (\text{A.5})$$

$$z_2 \cdot r_N = z_2^0 + v_2 \cdot \xi^* \quad (\text{A.6})$$

Where $z_1 = n_1/n_T$ and $z_2 = n_2/n_T$ are the global mole fractions of iC4(1) and C4(2), respectively, $z_1^0 = n_1^0/n_T^0$ and $z_2^0 = n_2^0/n_T^0$ are the initial global mole fractions of iC4(1) and C4(2), respectively, ξ^* is the extent of reaction relative to the initial total number of moles ($\xi^* = \xi/n_T^0$), and $r_N = n_T/n_T^0$. Notice that if $n_T^0 = 1$, then, $\xi^* = \xi$.

By adding Eqs. (A.5) and (A.6) and taking into account that $z_1 + z_2 = 1$ and $z_1^0 + z_2^0 = 1$, we write:

$$r_N = 1 + (v_1 + v_2) \cdot \xi^* \quad (\text{A.7})$$

Introducing the expression (A.7) into the Eqs. (A.5) and (A.6), we obtain:

$$z_1 = \frac{z_1^0 + \nu_1 \cdot \zeta^*}{1 + (\nu_1 + \nu_2) \cdot \zeta^*} \quad (11.1)$$

$$z_2 = \frac{z_2^0 + \nu_2 \cdot \zeta^*}{1 + (\nu_1 + \nu_2) \cdot \zeta^*} \quad (11.2)$$

From reaction (1), it should be clear that $\nu_1 = (+1)$ and $\nu_2 = (-1)$. Hence, Eqs. (A.1) and (A.2) become:

$$n_1 = n_1^0 + \zeta \quad (A.8)$$

$$n_2 = n_2^0 - \zeta \quad (A.9)$$

The numbers of moles n_1 and n_2 must be greater than or equal to zero. By combining the inequality $n_1 \geq 0$ with Eq. (A.8), and the inequality $n_2 \geq 0$ with Eq. (A.9), one obtains the bounds for ζ , i.e.,

$$\zeta_{min} = (-n_1^0) \quad (A.10)$$

$$\zeta_{max} = n_2^0 \quad (A.11)$$

Eqs. (A.10) and (A.11) imply that:

$$\zeta_{min}^* = (-1)(n_1^0/n_T^0) = (-1)(z_1^0) \quad (A.12)$$

$$\zeta_{max}^* = (n_2^0/n_T^0) = z_2^0 \quad (A.13)$$

The difference between these two bounds is the size of the possible variation range for ζ^* . Such interval length equals $(z_2^0 - (-1)(z_1^0)) = 1$. The bounds in Eqs. (A.12) and (A.13) are based only on the stoichiometry of reaction (1). Hence, they are conservative bounds.

APPENDIX B. Application of the SRK-EoS to the C4(2)+iC4(1) system when regarded as non-reactive

Table B.1 presents the values for the critical coordinates and acentric factor, for iC4(1) and C4(2), which were used in this work within the SRK-EoS [3]. Figure B.1 presents a vapor-liquid equilibrium diagram at 273.15 K, for the (regarded as non-reactive) system C4(2)+iC4(1). The predictions by the model, made for binary interaction parameters set to zero (solid lines), have a level of agreement with the experimental data (circles) which we consider sufficient in view of the goals of this work.

Table B.1. Pure component constants [6]

Compound	T_c (K)	P_c (bar)	ω
i-butane(1)	407.800	36.400	0.1835
n-butane(2)	425.120	37.960	0.2002

Literature cited

- [1] R.A. Asuquo, G. Eder-Mirth, J. A. Lercher. n-Butane isomerization over acidic mordenite. *J. of Catalysis*, 155, 376-382, 1995
- [2] A. Dhar, R. L. Vekariya, P. Bhadja. n-Alkane isomerization by catalysis—a method of industrial importance: An overview. *Cogent Chemistry* (2018), 4: 1514686
- [3] G. Soave, “Equilibrium constants from a modified Redlich-Kwong equation of state,” *Chem. Eng. Sci.*, vol. 27, no. 6, pp. 1197–1203, 1972.
- [4] M. Cismondi and M. L. Michelsen, “Global phase equilibrium calculations: Critical lines, critical end points and liquid-liquid-vapour equilibrium in binary mixtures,” *J. Supercrit. Fluids*, vol. 39, no. 3, pp. 287–295, 2007.
- [5] J. M. Smith, H. C. Van Ness, and M. M. Abbott, *Introduction to Chemical Engineering Thermodynamics*, 6th ed. New York: McGraw-Hill Chemical Engineering Series, 2001.
- [6] *DIPPR 801 Database. Evaluated Process Design Data*. Public Release in, American Institute of Chemical Engineers, Design Institute for Physical Property Data, BYU-DIPPR, Thermophysical Properties Laboratory: Provo, UT, 2003.
- [7] M.L. Michelsen and J.M. Mollerup, *Thermodynamic Modelling: Fundamentals and Computational Aspects*. Denmark: Tie-Line Publications, 2007.
- [8] S. B. Rodriguez-Reartes, M. Cismondi, and M. S. Zabaloy, “Computation of solid-fluid-fluid equilibria for binary asymmetric mixtures in wide ranges of conditions,” *J. Supercrit. Fluids*, vol. 57, no. 1, pp. 9–24, 2011.
- [9] J.M. Prausnitz, R.N. Lichtenthaler, E. Gomes de Azevedo. *Molecular Thermodynamics of Fluid-Phase Equilibria* (3rd Edition) (Prentice Hall International Series in the Physical and Chemical Engineering Sciences) (1999)
- [10] R.L. Scott and P.H. Van Konynenburg, “Static properties of solutions. Van der Waals and related models for hydrocarbon mixtures,” *Discuss. Faraday Soc.*, vol. 49 (1970), pp. 87–97, 1970.
- [11] M. Hirata and S. Suda, “Equilibrium Measurements by the Vapor-Liquid Flow Method,” *Bull. Japan Pet. Inst.*, vol. 10, pp. 20–27, 1968.

FIGURES

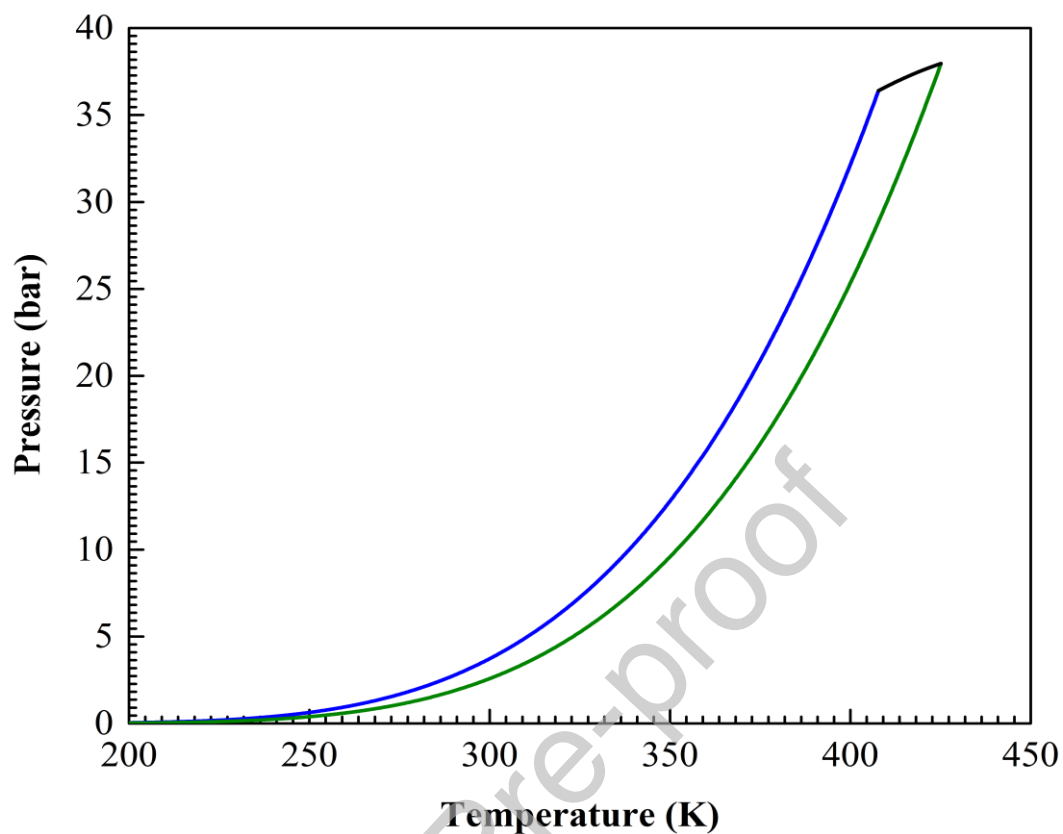


Figure 1. Pressure – temperature projection of the calculated non-reactive binary fluid phase equilibrium characteristic map (B-CM) of the C4(2) + iC4(1) system. Solid black line: critical locus. Solid blue and green lines: pure component vapor-liquid equilibrium curve for iC4(1) and C4(2) respectively. Model: SRK-EoS with QMRs and $k_{ij}=0$ and $l_{ij}=0$.

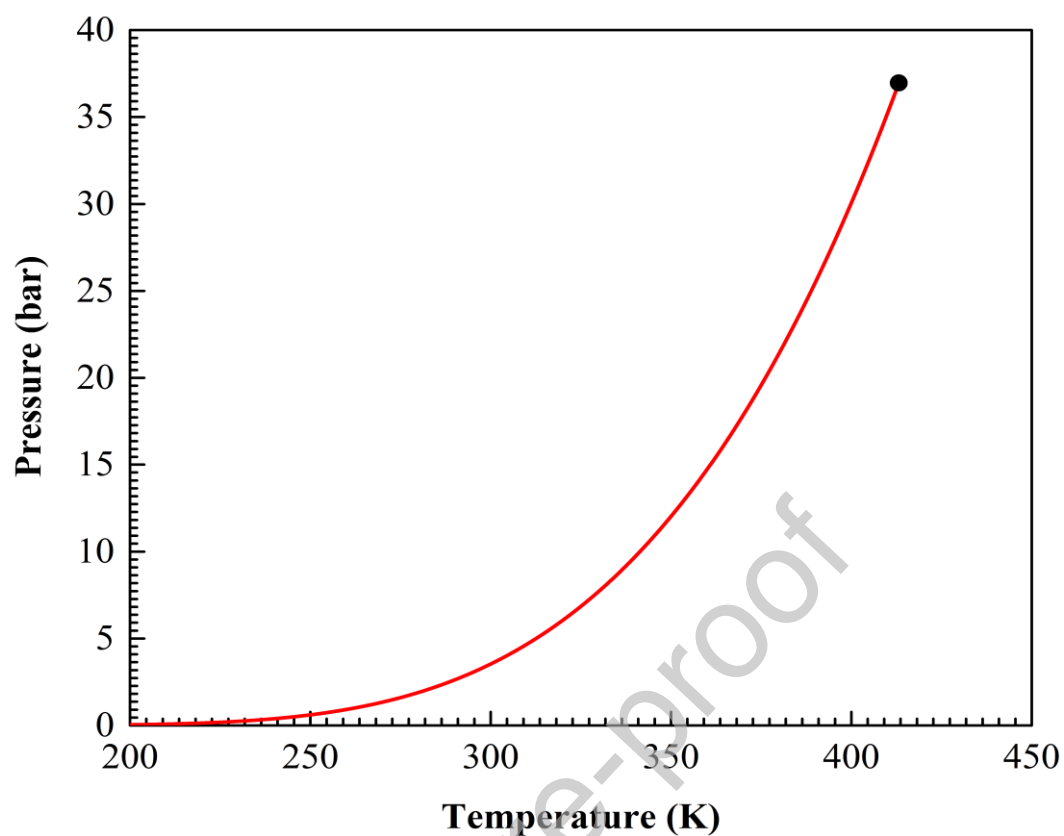


Figure 2. Pressure – Temperature projection of the calculated fluid phase equilibrium characteristic map of the C4(2) + iC4(1) reactive system (B-R-CM). Red line: reactive VLE curve. ●: Reactive critical point. Model: SRK-EoS with QMRs and $k_{ij}=0$ and $l_{ij}=0$.

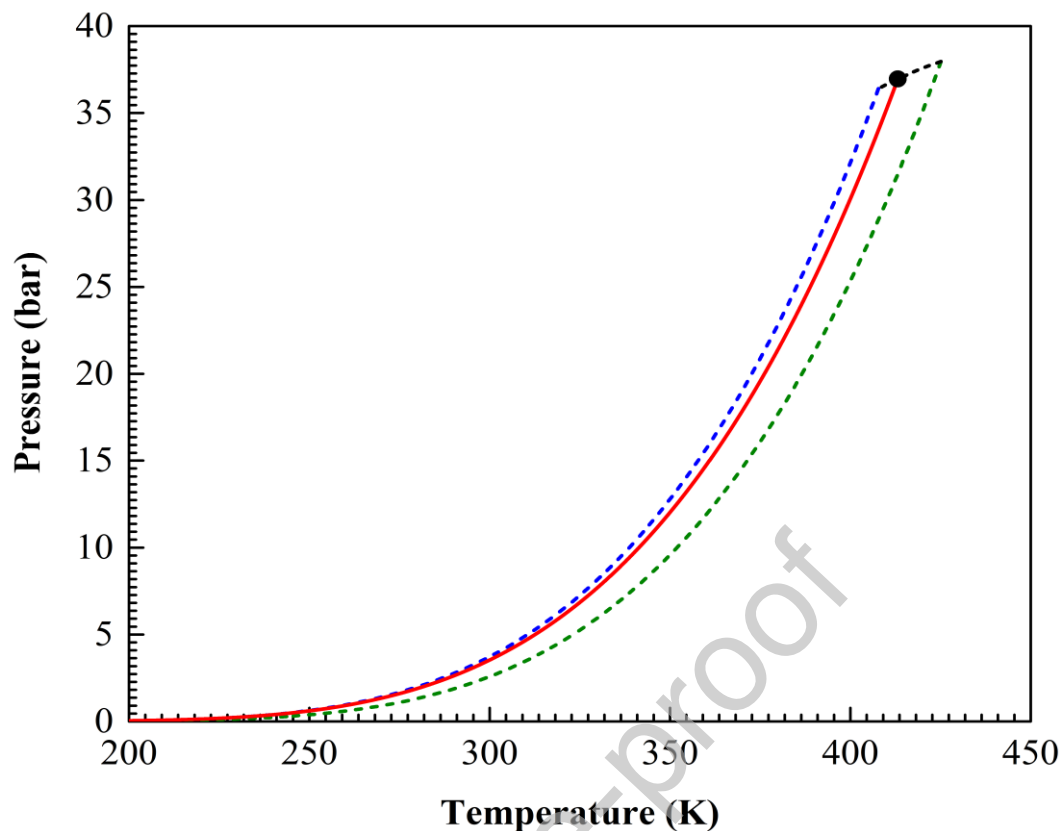


Figure 3. Pressure – Temperature projection of the calculated B-CM and B-R-CM of the C4(2) + iC4(1) system. Red line: reactive VLE curve. ●: Reactive critical point. Dashed black line: critical locus of the C4(2) + iC4(1) non-reactive system. Dashed blue and green lines: pure component saturation curves for iC4(1) and C4(2), respectively. Model: SRK-EoS with QMRs and $k_{ij}=0$ and $l_{ij}=0$.

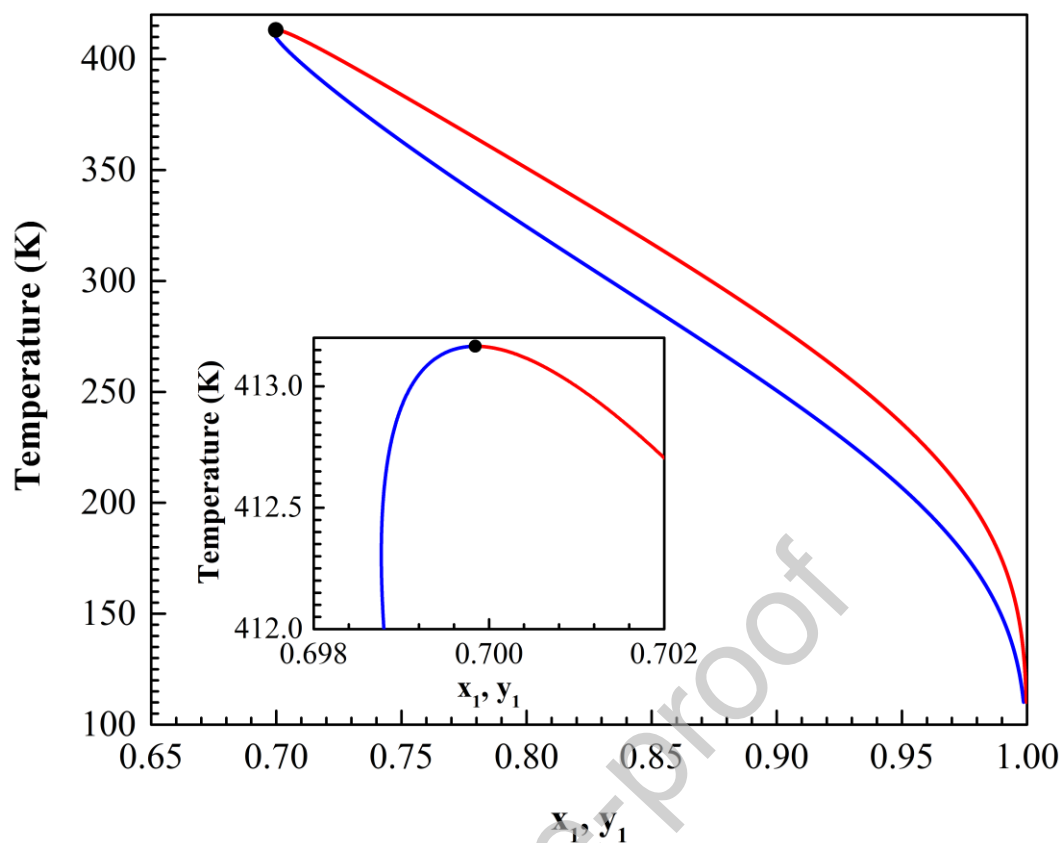


Figure 4. Temperature – composition projection of the calculated fluid phase equilibrium characteristic map of the C4(2) + iC4(1) reactive system. Red line: saturated vapor (T vs y_1). Blue line: saturated liquid (T vs x_1). ●: Reactive critical point. Model: SRK-EoS with QMRs and $k_{ij}=0$ and $l_{ij}=0$.

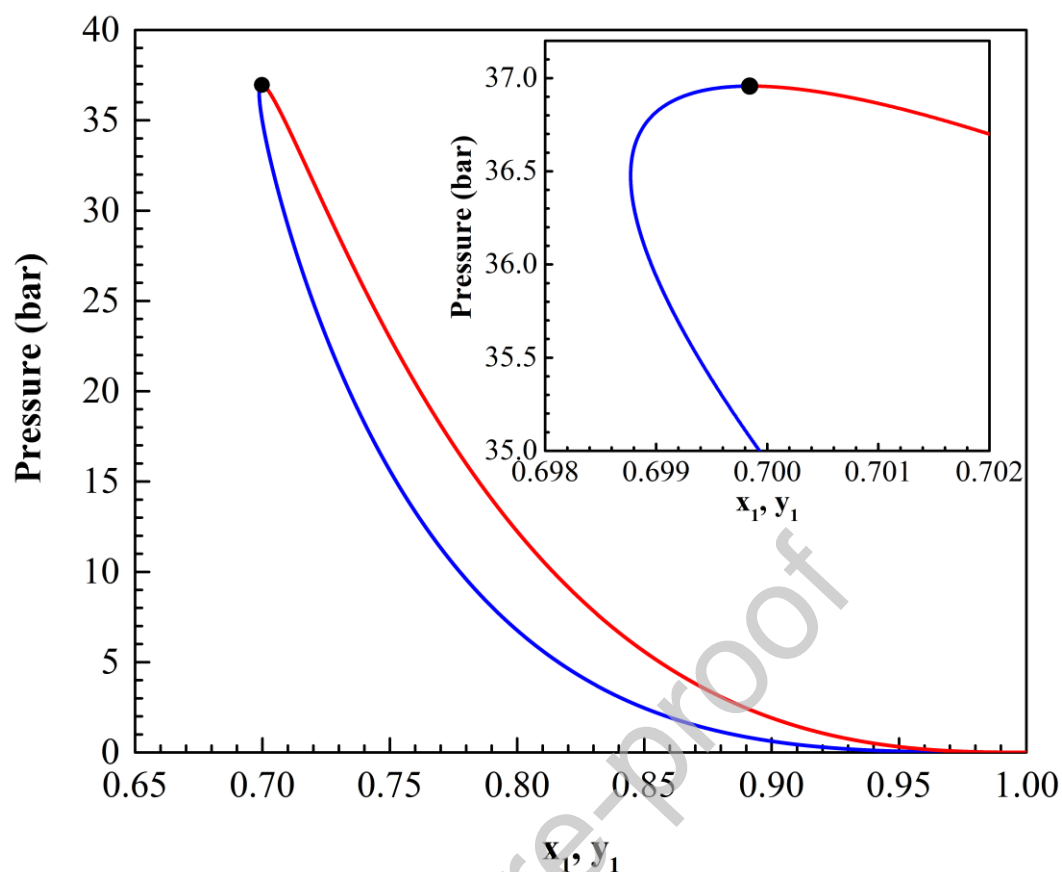


Figure 5. Pressure – composition projection of the calculated fluid phase equilibrium characteristic map of the C4(2) + iC4(1) reactive system. Red line: saturated vapor (P vs y_1). Blue line: saturated liquid (P vs x_1). ●: Reactive critical point. Model: SRK-EoS with QMRs and $k_{ij}=0$ and $l_{ij}=0$.

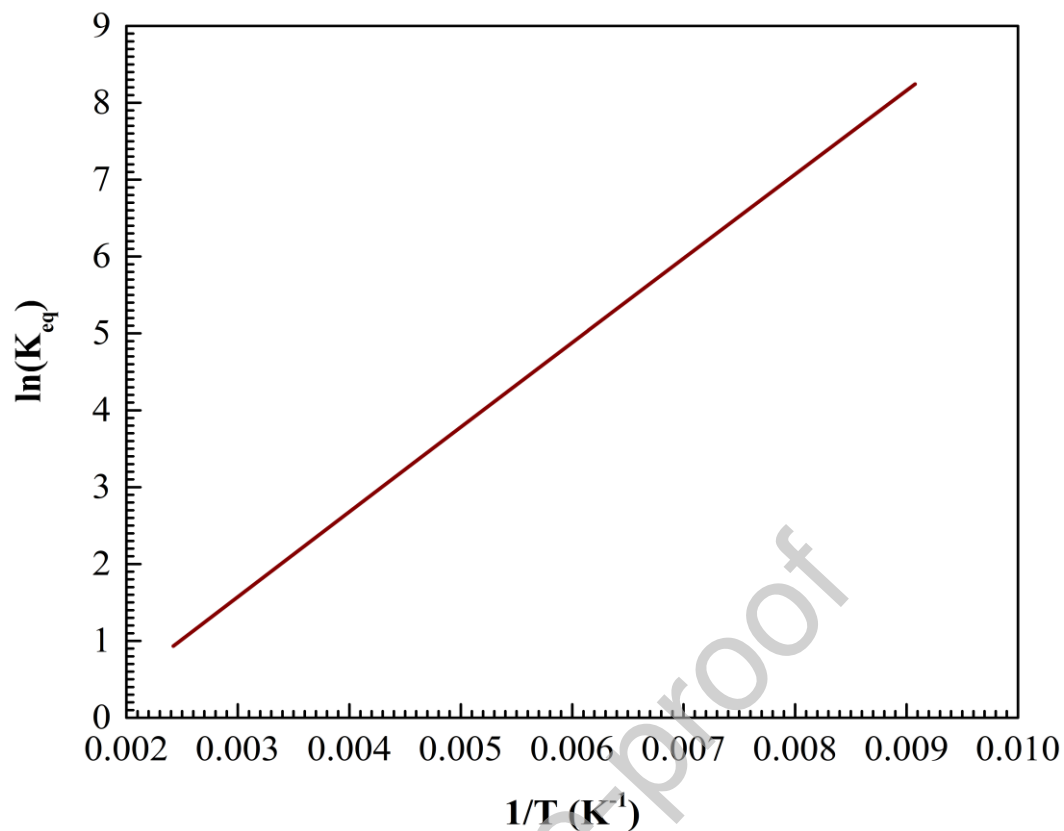


Figure 6. Computed equilibrium constant as a function of inverse temperature for the isomerization reaction of C4(2) to iC4(1). Model: SRK-EoS with QMRs and $k_{ij}=0$ and $l_{ij}=0$.

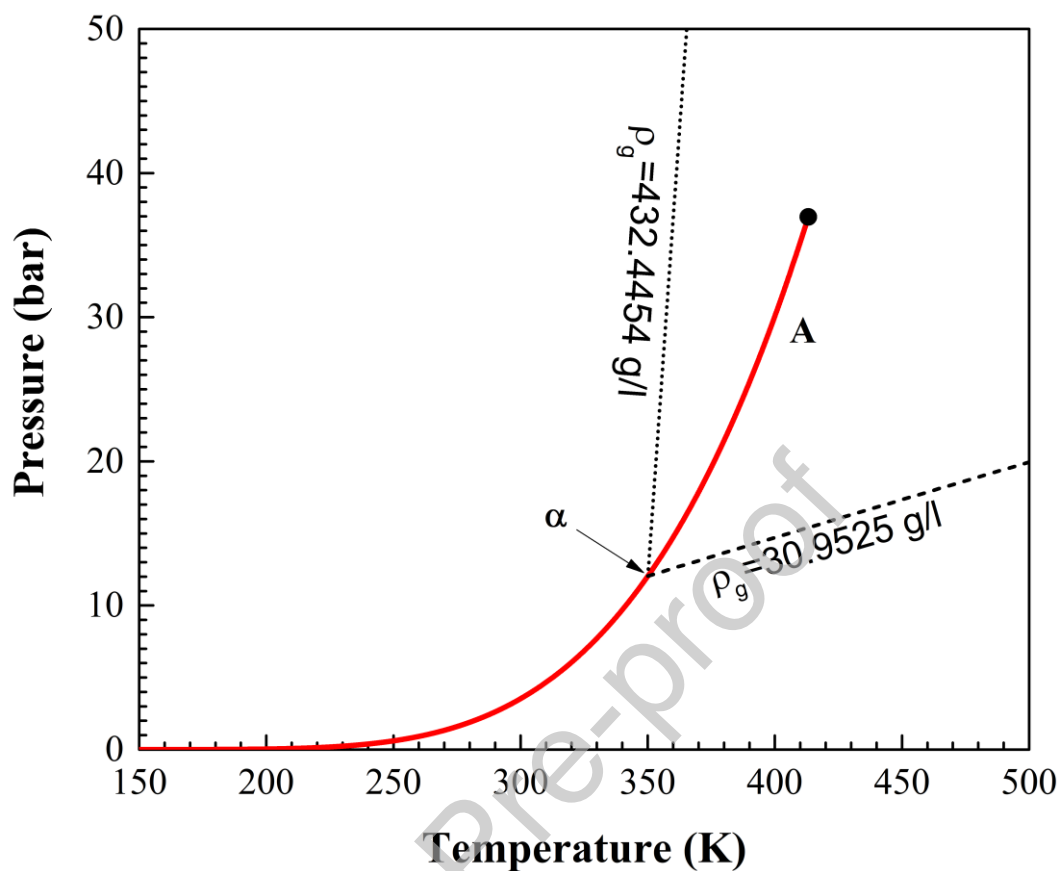


Figure 7. Pressure - Temperature projection of the calculated fluid phase equilibrium characteristic map of the C4(2) + iC4(1) reactive system (B-R-CM). Red line: reactive VLE curve (=locus A). •: Reactive critical point. Dotted black line and dashed black line: computed reactive isochores. Model: SRK-EoS with QMRs and $k_{ij}=0$ and $l_{ij}=0$. ρ_g is the reactive isochore global mass density.

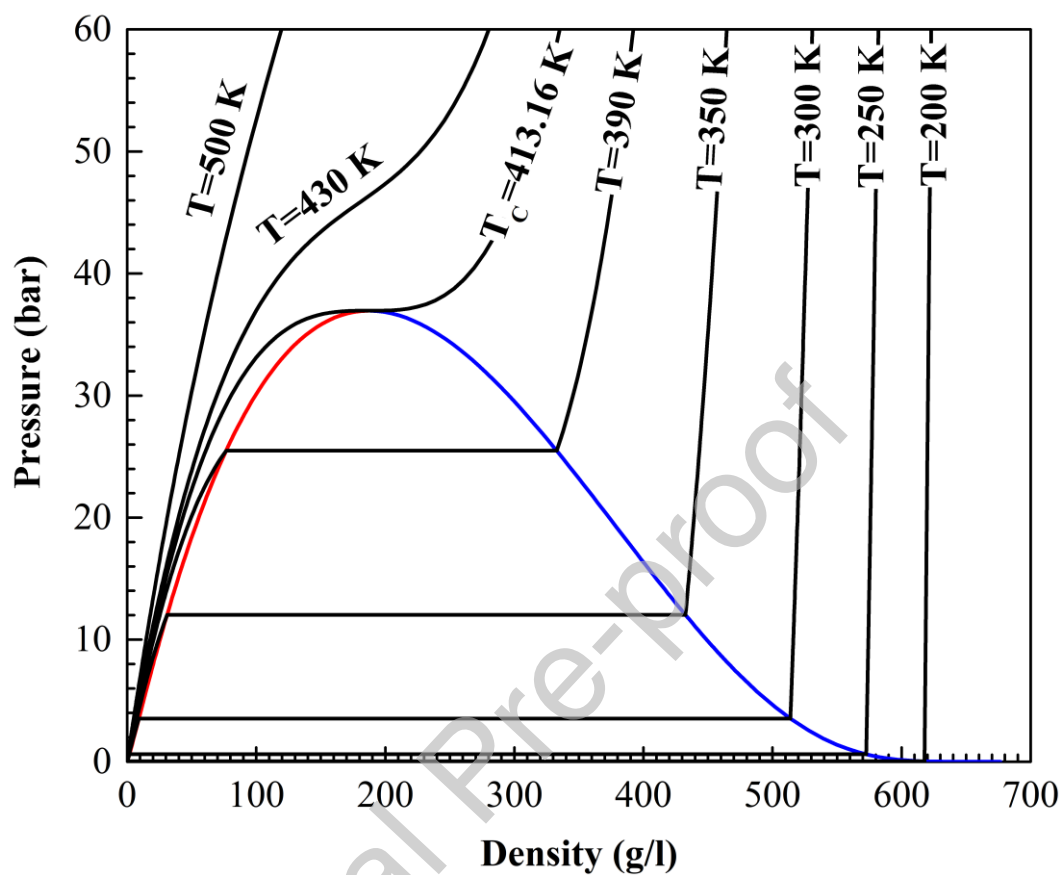


Figure 8. Pressure - saturated mass density projection of the calculated C4(2) + iC4(1) B-R-CM. Red line: saturated vapor. Blue line: saturated liquid. Solid black lines: computed reactive isotherms. Model: SRK-EoS with QMRs and $k_{ij}=0$ and $l_{ij}=0$.

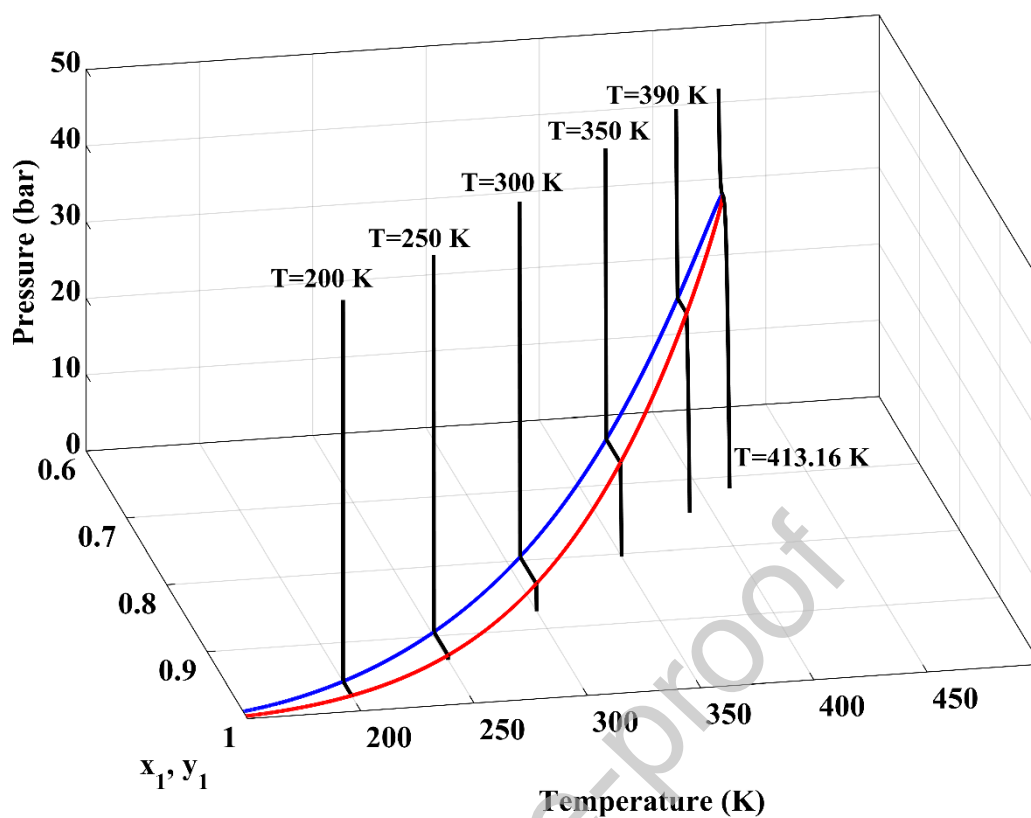


Figure 9a. Pressure – temperature – composition projection of the calculated C4(2) + iC4(1) B-R-CM. Red line: saturated vapor (y_1). Blue line: saturated liquid (x_1). Solid black lines: computed reactive isotherms. Model: SRK-EoS with QMRs and $k_{ij}=0$ and $l_{ij}=0$.

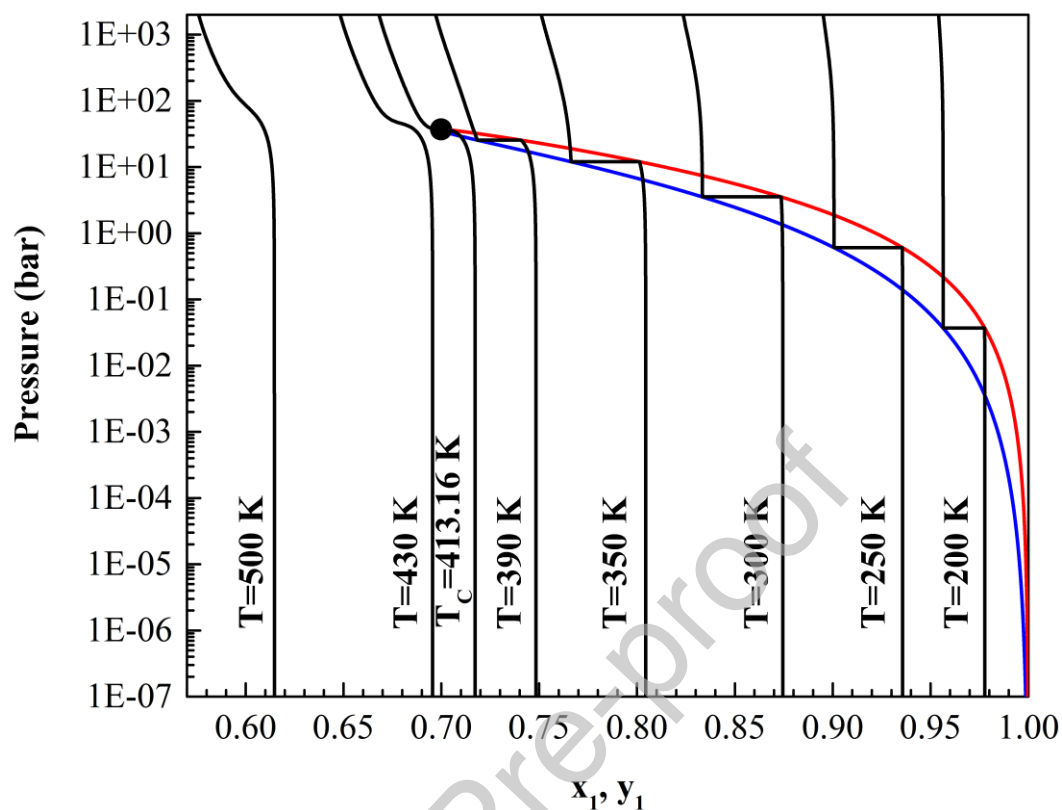


Figure 9b. Pressure – composition projection of the calculated fluid phase equilibrium characteristic map of the C4(2) + iC4(1) reactive system. Red line: saturated vapor (P vs y_1). Blue line: saturated liquid (P vs x_1). ●: Reactive critical point. Solid black lines: computed reactive isotherms. Model: SRK EoS with QMRs and $k_{ij}=0$ and $l_{ij}=0$.

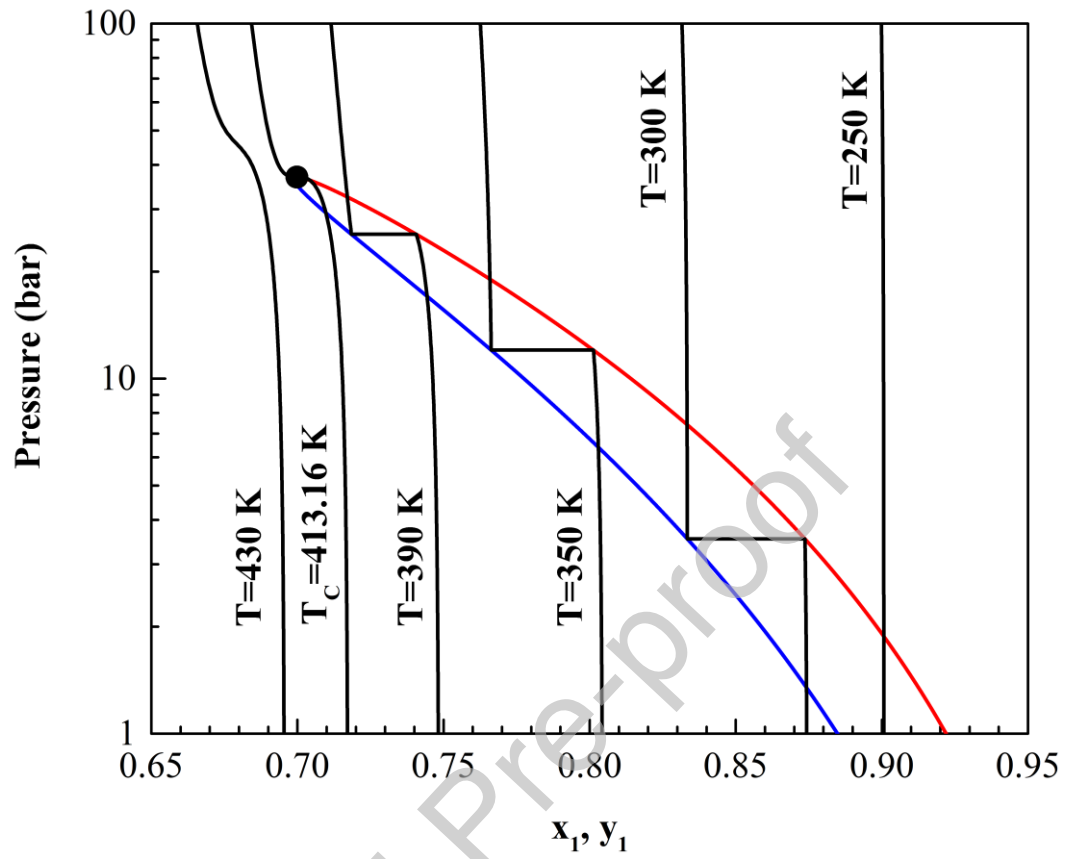


Figure 9c. Zoom of Fig 9b.

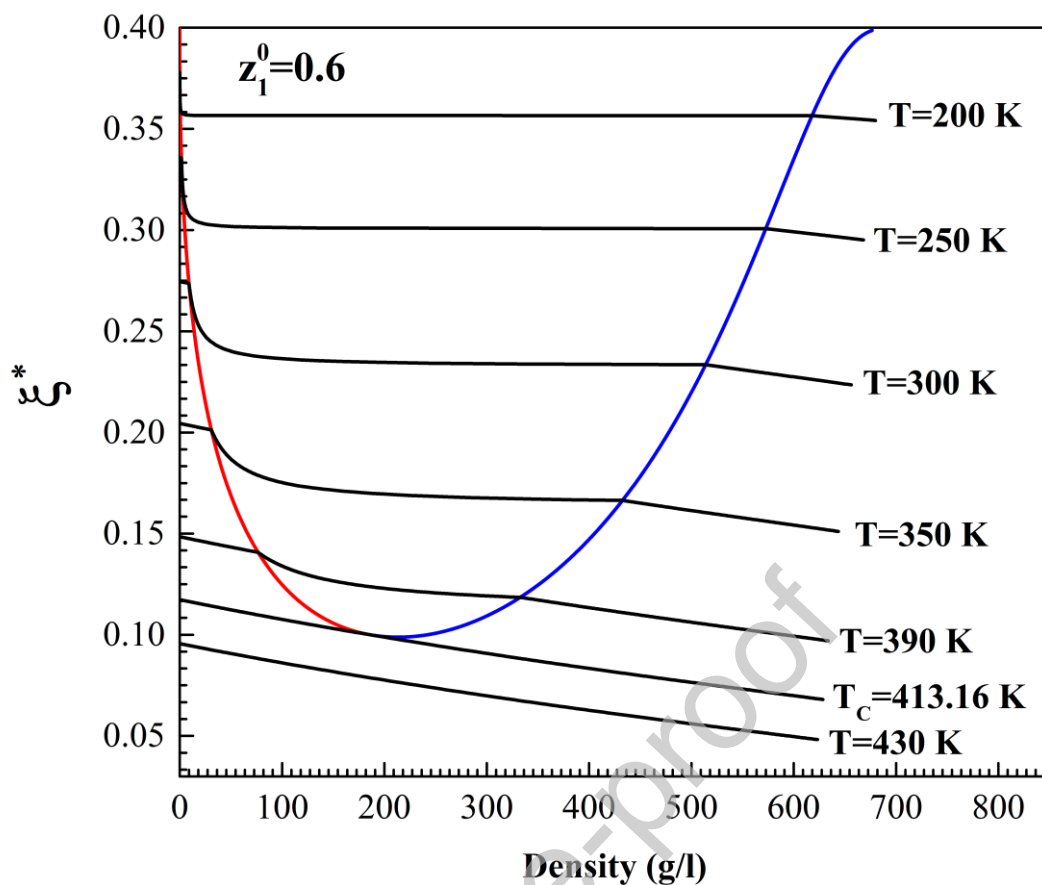


Figure 10. Calculated ξ^* versus overall mass density (ρ_g) for the C4(2) + iC4(1) reactive system with $z_{iC4}^0=0.60$ at varying temperatures. Solid black lines: Computed isotherms for $z_{iC4}^0=0.60$. Red line: overall density equal to computed saturated vapor density at the set T . Blue line: overall density equal to computed saturated liquid density at the set T . Model: SRK-EoS with QMRs and $k_{ij}=0$ and $l_{ij}=0$.

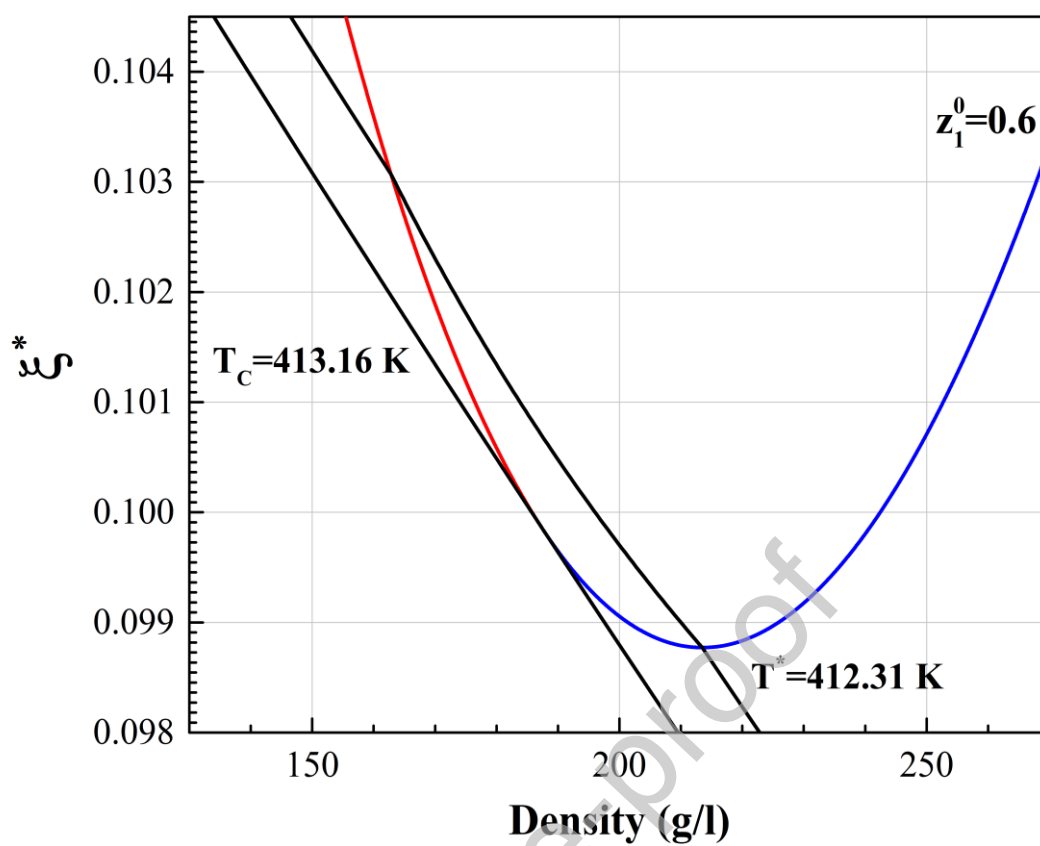


Figure 11. Zoom of Fig. 10 but showing only two isotherms (one of them was not shown in Fig. 10).

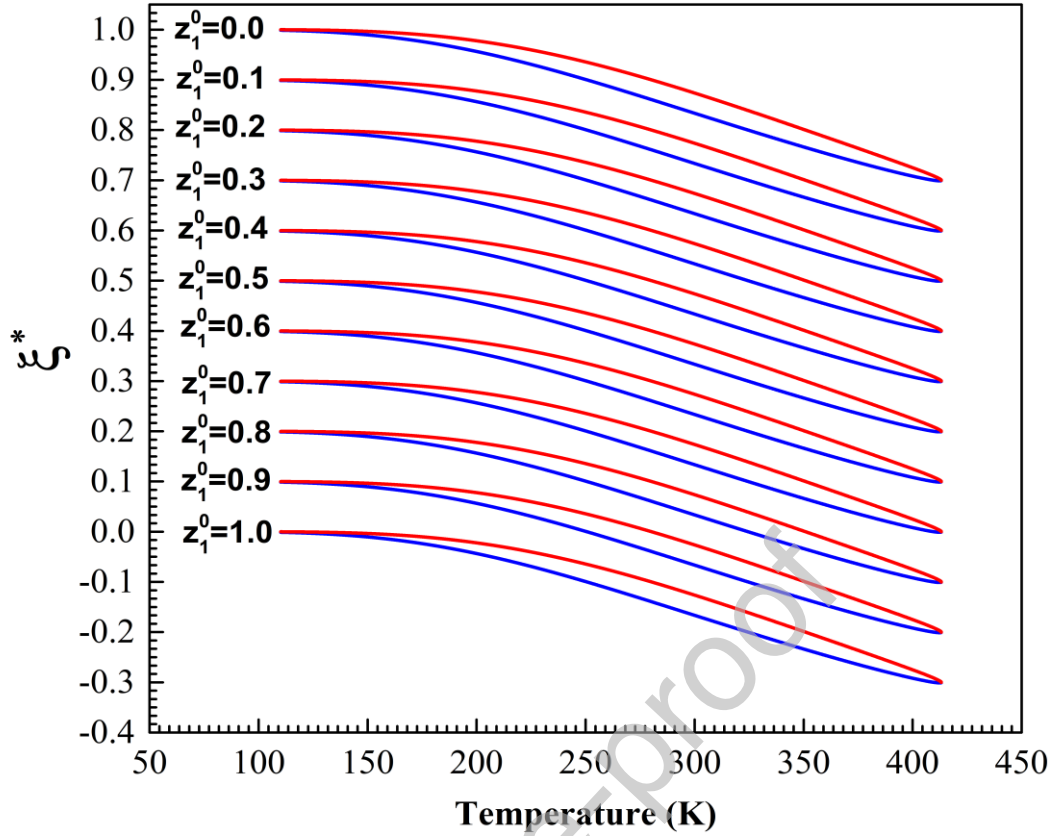


Figure 12. ξ^* at saturation versus temperature, at varying initial global composition (z_{iC4}^0), calculated for system C4(2) + iC4(1). Red lines: saturated vapor. Blue lines: saturated liquid. Model: SRK-EoS with QMRs and $k_{ij}=0$ and $l_{ij}=0$.

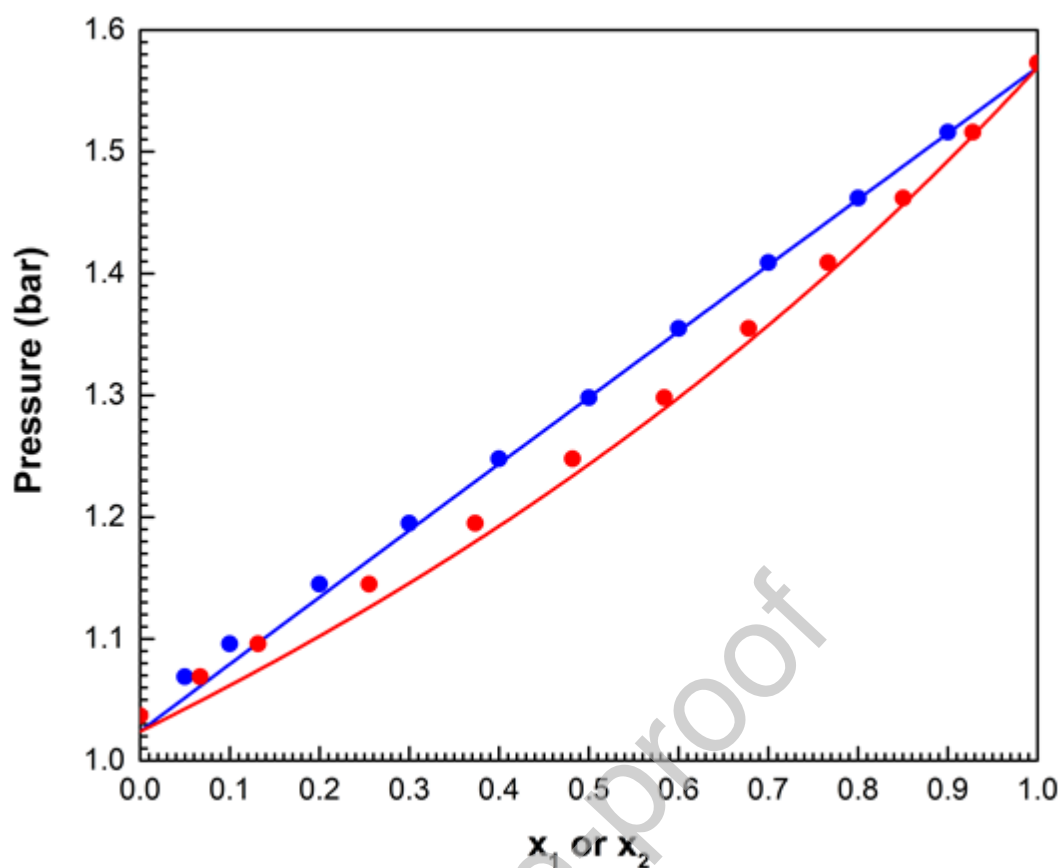


Figure B.1. Isothermal (non-reactive) vapor-liquid equilibrium diagram for the system isobutane (1) + n-butane (2). Temperature = 273.15 K. Solid lines: computed bubble (blue) and dew (red) lines. Circles: experimental data taken from reference [11]. Model: SRK EoS with QMRs and $k_{ij}=0$ and $l_{ij}=0$ and pure component constants from Table B.1.